

Charge Dynamics and Storage Behaviors of Ionic Liquids/Ionomer Electrolyte in Electroactive Devices

Jun-Hong Lin and Ming-Tse Lee

Abstract—Developing advanced electroactive devices requires the understanding of the influence of sample geometry on the charge transport and storage. In these devices both diffusion and drift processes depend on the distances over which ions travel. In this paper the charge dynamics of Aquivion membrane with 40 wt% uptake of EMI-Tf (1-ethyl-3-methylimidazolium trifluoromethane -sulfonate) cells were investigated over a broad membrane thickness (d) range. It was found that the double layer charging time τ_{DL} is linearly proportional to the thickness (d) for all applied voltages. However, in the longer time regimes ($t \gg \tau_{DL}$) under a high applied voltage (>0.5 V) where the significant charge storage occurs, it was found that the relationship between charge storage and applied voltage becomes nonlinear and also the longer time charging response of $\tau_{diff} = d^2 / (4D)$, corresponding to the ion diffusion, was not observed.

Index Terms—Ionic liquids, ionomer, capacitance, electroactive devices.

I. INTRODUCTION

Ion transport and storage in ionomer membranes are of great interest for electroactive devices, such as actuators, sensors, energy harvesting devices, and supercapacitors [1]-[3]. In general, charge transport is a result of drift and diffusion, described by the ion mobility μ , diffusion coefficient D , and mobile ion concentration n . μ and D are related through the Einstein equation [4]-[6]. During charging, ions in the electrolyte move towards electrodes of opposite polarity due to electric field between charged electrodes created by applied potential which is equivalent to potential drop at the two electrodes as illustrated in Fig. 1(a). For the metal-ionic conductor-metal (MIM) system of Fig. 1(a) under a step voltage (from 0 V at $t < 0$ to V volts at $t > 0$), the initial current before the screening of electric field in the films occurring is $I_0 = \sigma VS/d$, where $\sigma (=qn\mu)$ is the conductivity, d is the membrane thickness, and S is the electrode area. When the applied voltage is not high (eV is not too high compared with kT , where k is the Boltzmann's constant), the initial transient current follows the charging of electric double layer capacitors C_D in series with a bulk resistor R_{bulk} (see Fig. 1(b)) [6]-[8],

$$I(t) = I_0 \exp(-t/\tau_{DL}) \quad (1)$$

Manuscript received October 21, 2013; revised January 13, 2014. This work was supported in part by the National Science Council of National Science Council of the Republic of China, Taiwan, under Grant NSC 102-2218-E-151-003.

Jun-Hong Lin and Ming-Tse Lee are with the Department of Mold and Die Engineering, National Kaohsiung University of Applied Sciences, Kaohsiung, Taiwan, Republic of China (e-mail: jhlin@kuas.edu.tw, 1101316155@kuas.edu.tw).

where $\tau_{DL} = d \lambda_D / 2D = RC_D$, describes the typical charging time for the electric double layer which has a thickness λ_D , the Debye length,

$$\lambda_D = (\epsilon \epsilon_0 kT / Z^2 e^2 n)^{1/2} \quad (2)$$

where Z is the mobile ion charge ($=1$ for the ionic liquids investigated in this paper), and $q=e$, electron charge. It is also noted that our recent study shows that for the ionic systems investigated here, this model is still valid for applied voltage at least up to 1 volts.

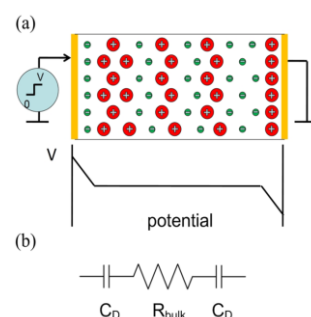


Fig. 1. (a) Schematics of an electrolyte containing film sandwiched between metal electrodes under an applied voltage. Schematic of the voltage drop across the film after it is charged, illustrating that most voltage drop occurs near the blocking electrodes where the mobile ions screen the charges in the metal electrodes. (b) The equivalent circuit of ionic film metal system where R_{bulk} is the bulk resistance of the film and CD is from the electrical double layer.

From the classical picture of the ionic system, in the initial charging process the mobile charges were driven to form electric double layers on the electrodes and this charging time is equal to $\tau_{DL} = RC = \lambda_D d / (2D)$ [4]-[7], [9]. As a result, there is a charge deficient region near the interface which will be filled by ion diffusion from the bulk. Several theoretical models have predicted that this later diffusion process has a time constant $\tau_{diff} = d^2 / (4D)$ which is much larger than τ_{DL} since $d \gg \lambda_D$ [4], [5], [7], [8]. For most ionic electroactive devices, the response time is much longer than τ_{DL} , which is $\ll 10^{-2}$ seconds for the films studied here, and substantial actions and device functions occur during this later stage of the charging process near the electrode. Hence, one critical question is whether by reducing the ionic conductor thickness d , a much fast device response speed can be achieved if $\tau_{diff} = d^2 / (4D)$. A fast device response is highly desired for almost all the electroactive devices.

This paper investigates the influence of the ionomer membrane thickness d (in thickness ranging from 0.8 μm to 20 μm) with various applied voltages on the ion transport and storage processes for the ionomer of Aquivion with 40 wt% ionic liquids (ILs) of EMI-Tf (1-ethyl-3-methylimidazolium trifluoromethanesulfonate). Ionic liquids (ILs), which are a class of salt in liquid form that containing both ions and

neutral molecules, are used here as electrolytes because of many interesting properties that make them very attractive for ionic electroactive polymer (EAP) devices [10]-[12]. For example, the vapor pressure of ionic liquids is negligibly low and as a result they will not evaporate out of the EAP devices when operated in ambient condition. It has been demonstrated that comparing to water the use of ILs as solvent for EAP actuators can dramatically increase the lifetime of transducer [13], [14]. Their high mobility leads to potentially fast response of EAP devices while the wide electro-chemical window ($\sim 4V$) allows for higher applied voltages [1]-[3], [10]-[12]. Both cations and anions are present in ionic liquids and for the study here, it is assumed $n_+ = n_-$ (the subscripts + and - indicate positive and negative charges).

Our earlier study have shown that 40wt% EMI-Tf is above the critical IL uptake where the conductivity of the ionomer/IL membrane exhibits much higher conductivity than that of the pure ionomer [15]. The experimental results reveal that over a broad thickness range, the initial charge dynamics can be described well by the RC circuit model where the resistance R is determined by the bulk conductivity of the ionic conductors and C is determined by the Debye length, which does not change with the membrane thickness d. Consequently, τ_{DL} increases linearly with the ionomer thickness or the gap width between the anode and cathode d. On the other hand, experimental results reveal that for the systems studied, the later stage charge responses display voltage dependence. Under 0.1 V applied step voltage, the charging process seems to follow d^2 thickness dependence, while for data acquired at 0.5 V and higher, the charge diffusion time becomes progressively shorter with increased voltage than that predicted from $\tau_{diff} = d^2 / (4D)$, suggesting that the mobile charges diffusing to the interface at later stage is mainly from a region at a distance much shorter than $d/2$ for membranes.

II. EXPERIMENTAL

Aquivion (Hyflon) is chosen for this study since it is known in the literature as short side chain ionomer (in comparison to Nafion that is indicated as long side chain ionomer) which may be more desirable compared with normally used Nafion for ionic EAP actuators [14]-[20]. These perfluorosulfonate ionomers consist of a polytetrafluoroethylene (PTFE) backbone and double ether perfluoro side chains terminating in a sulfonic acid group as illustrated in Fig. 2. Aquivion (EW830) solution, and 1-ethyl-3-methylimidazolium trifluoromethanesulfonate (EMI-Tf) are purchased from Solvay Solexis and Aldrich, respectively. EMI-Tf is chosen because of high conductivity ($8.6 \times 10^{-3} S/cm$), low viscosity (45 cP at 298K) and larger electrochemical window (4.1 V). It is one of the commonly used ionic liquids in ionic polymer actuators [13], [15]-[17], [21], [22]. All the materials were dried in vacuum at $80^\circ C$ to remove moisture before processing and characterization.

Aquivion solution blend with 40wt% uptake of EMI-Tf are prepared and then diluted by N-Methyl-2-pyrrolidone (NMP) solvent with ratio of 1:3 for thicker films (11 and 20 μm thick) and 1:8 for thinner films (0.8 and 1.9 μm thick). Films are solution cast on metalized Si substrates. In this study, Si/Ti/Au substrate is prepared by e-beam evaporator with the

electrode area of $1mm^2$. Film thickness is controlled by the amount of mixture casted on the substrate. After drying at $96^\circ C$ for 10 hrs, the film is annealed at $150^\circ C$ for 2hrs followed. To form metal-ionomer-metal (MIM) sample system, 30 nm thick gold film is deposited as the top electrode.

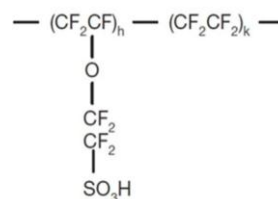


Fig. 2. Molecule structure of short side chain Aquivion ionomer (EW830).

The electrical measurement was carried out in a sealed metal box with desiccant inside to prevent the absorption of moisture. The box is equipped with a thermocouple to monitor the temperature during the measurement. The impedance spectroscopy was measured by a potentiostat Princeton 2237. The dc conductivity was calculated by $\sigma = d/RS$, where R is determined from the Nyquist plot (see Fig. 3(a)) [15], [17]. To obtain the dielectric constant of the membranes, the samples were cooled down in an environment chamber (Versa Tenn III) to reduce the conductivity of the MIM system so that the dielectric constant before the screening of the applied field occurs, at frequencies $\gg 1/\tau_{DL}$, can be measured within the frequency window of the set-up which is below 1 MHz. In contrast to the conductivity which decreases with temperature the dielectric constant of the ionomers only very weakly temperature dependent and the value thus acquired can be used for room temperature [23]-[25]. The transient current vs. time was acquired by a potentiostat (Princeton 2237) which output was connected to a high sampling rate oscilloscope to collect data during the fast charging process ($< 1 \mu s$). The applied voltage is from 0.1 V to 4 V. The accumulation of blocked charges on membrane electrodes and the charge imbalance in the membrane may affect the electrical measurement. Therefore, several cycles of Cyclic Voltammetry (CV) scan with a low voltage ($< 1 V$) and high scan rate were performed to help cleaning the electrode surface then the samples were shorted for at least 30 min to ensure that the charges redistribute to the equilibrium state as possible [26].

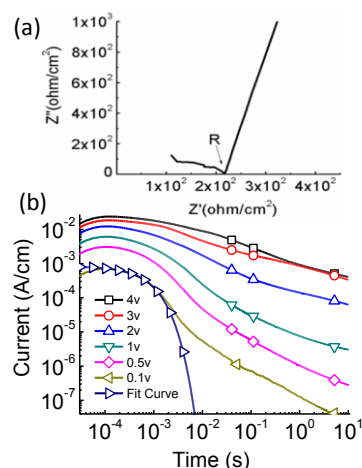


Fig. 3. (a) The Nyquist plot used to determine the membrane resistance R and (b) the current density and fitting (0.1V) to Eq. (1) of the 11 μm thick Aquivion membrane with 40 wt% uptake of EMI-Tf under various step voltages.

III. EXPERIMENTAL RESULTS AND DISCUSSION

The current responses of Aquivion with 40 wt% EMI-Tf uptake under various step voltages (from 0.1 V to 4 V) were characterized for membranes of 0.8 μm , 1.9 μm , 11 μm , and 20 μm thick to investigate the influence of the membrane thickness d on the charge dynamics of this MIM system. Fitting of the transient current data (as illustrated in Fig. 3b) yields σ , μ , λ_D , τ_{DL} for this MIM system (summarized in Table I). Fig. 4 presents the charge density with time acquired under 0.1V and 2V step voltages for membranes of different thicknesses. The charge response time τ_{DL} (see Eq. (1)) for films of 1.9 μm , 11 μm , and 20 μm thick is also indicated in the Fig. 4 labeled as τ_1 (2.49×10^{-4} s), τ_2 (7.25×10^{-4} s), and τ_3 (1.29×10^{-3} s), respectively. The data show that the charge dynamic at a short time scale is controlled by the charging of electrical double layer and C_D does not change with film thickness and voltage studied here.

The data for the membranes of 0.8 μm thick display a very different behavior where the current becomes much larger than that in other films. It is likely that there is a significant leakage current in such a thin film, which superimposes on the regular diffusion and drifting currents. As illustrated in Fig. 1(a), due to the electric double layer, most voltage drop occurs within the Debye length near the electrodes, which is about 1 nm for the MIM systems studied here. Hence, the field level in the interface region can reach ~ 0.1 GV/m or larger, which could induce strong charge injection from the electrodes. For thick membranes, the bulk resistance limits the current flow, resulting in low leakage current (the current flow is bulk limited). While for thin membranes, this bulk resistance becomes small (the currents due to diffusion and drifting in the bulk region also become large) and consequently the current flow is interface limited, causing high leakage current as observed. The high leakage current in 0.8 μm thick membranes makes it difficult to perform quantitative data analysis and to deduce μ , τ_{DL} , λ_D , etc.

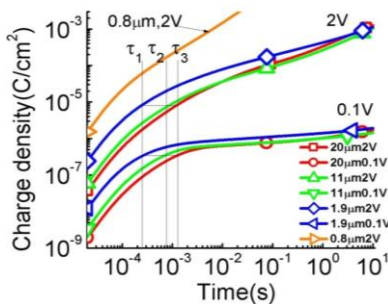


Fig. 4. The charge density as a function of time for the Aquivion film with 40 wt% uptake of EMI-Tf under 0.1 V and 2 V at the membrane thickness of $d = 0.8\text{m}$, 1.9m, 11m, and 20m. The abnormal high charge response of 0.8m sample may be a result of the high leakage current due to the reduction of the bulk thickness. The error bar is indicated by the size of the symbols in the figure.

The capacitance $C=Q/V$, where Q is the stored charge and V is the applied voltage on the two electrodes, measured under 0.1 V and 2 V for the membranes with various thicknesses as a function of time are shown in Fig. 5. As can be seen, the capacitances at the time below that for the charging of Debye layer (τ_{DL}) are nearly the same for the membranes of 1.9 μm , 11 μm , and 20 μm , which is consistent with the transient current data in Fig. 4. For membranes of 0.8 μm thick, the

high leakage current causes a very large apparent capacitance which increases with time and is typical for the capacitance due to space charge effect.

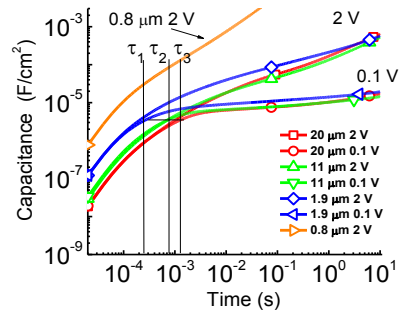


Fig. 5. The capacitance as a function of time for the Aquivion film with 40 wt% uptake of EMI-Tf under 0.1 V and 2 V step voltages. The error bar is indicated by the size of the symbols in the figure.

We now examine the current and charge responses at a longer time beyond τ_{DL} which is the time domain for most practical ionic electroactive devices to display large responses [12], [13], [19], [22], [23]. As revealed in Fig. 4, in contrast to the strong thickness dependence observed for τ_{DL} , the later stage current responses seem not to exhibit significant change with the membrane thickness when the membrane thickness d is reduced from 20 μm to 1.9 μm (except for the membranes of 0.8 μm thick). In Table I, $\tau_{diff} = d^2/(4D)$ is also listed which is 0.15 seconds for 1.9 μm thick film and increases to 15.6 seconds for 20 μm thick film. In order to display data more clearly and compare them with τ_{diff} directly, the charge density of these films is plotted against t/d^2 as presented in Fig. 6. The data show that under 0.1 V, the later stage charging process seems not to deviate significantly from the d^2 dependence at the reduced time interval between 10^{-4} and 10^{-1} (t/d^2). However, for higher voltages, the data deviate from the d^2 dependence markedly. At applied voltage >1 V, the data show that the charging time for films of 11 μm and 20 μm becomes much shorter than the d^2 dependence, compared with films of 1.9 μm thick membrane.

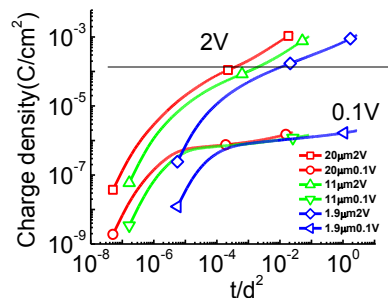


Fig. 6. The charge density as a function of t/d^2 for the Aquivion film with 40 wt% uptake of EMI-Tf under 0.1V, and 2 V at the membrane thickness of $d = 1.9\text{m}$, 11m, and 20m. The error bar is indicated by the size of the symbols in the figure.

Also we investigate the charging response of the electroactive device under various applied voltages. Sample of the Aquivion film with 40 wt% uptake of EMI-Tf with thickness ($d=11 \mu\text{m}$) membrane was selected for the discussion due to its proper diffusion time constant ($\tau_{diff} = d^2/4D=4.86$ seconds) for our experimental window which is below 10 seconds. Fig. 7 (a) presents the charge density as a function of time for the Aquivion film with 40 wt% uptake of EMI-Tf under 0.025V, 0.1V, 0.5V, 1V, 2V, 3V, and 4V. As

can be seen in Fig. 7 (a), the charging process consists of a fast charging process at the initial time scale ($t < \tau_{DL} = \tau_2 = 7.25 \times 10^{-4}$ s) leading to a fast raising regime in the plot and followed by a slow diffusion charging process resulting in a plateau regime at the longer time scale ($t \gg \tau_{DL}$).

Hence, we are interested in how the capacitance in response to the applied voltage against time of the device. Fig. 7 (b) plots the capacitance of the device against time under 0.025V, 0.1V, 0.5V, 1V, 2V, 3V, and 4V. The capacitance was deduced by the relation $C=Q/V$. As can be seen in Fig. 7(b), the device at $t=\tau_{DL}$ shows the same capacitance value $C_D=3.6 \times 10^{-6}$ (F/cm²) for all applied voltages. However, at the longer time regime ($t \gg \tau_{DL}$), the value of capacitance raises up dramatically with increased applied voltages.

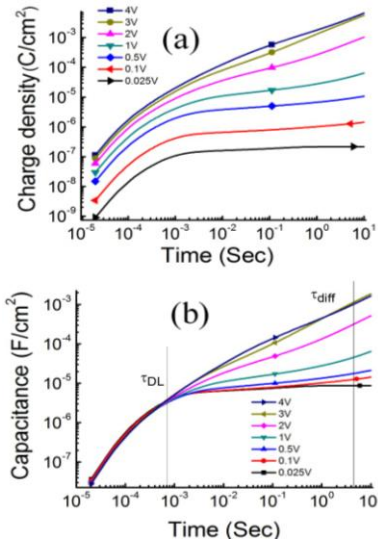


Fig. 7. (a) The charge density and (b) the capacitance as a function of time for the Aquivion film with 40 wt% uptake of EMI-Tf under 0.025V, 0.1V, 0.5V, 1V, 2V, 3V, and 4V at the membrane thickness of $d=11$ m.

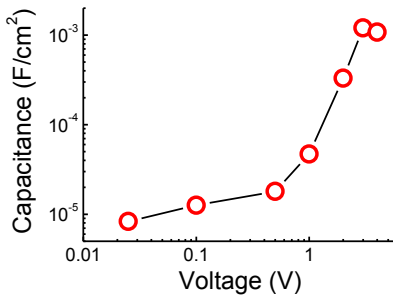


Fig. 8. The capacitance as a function of voltage for the Aquivion film with 40 wt% uptake of EMI-Tf at the membrane thickness of $d=11$ m.

TABLE I: SUMMARY OF D , D_L AND D_{DIFF} FOR THE AQUIVION MEMBRANES WITH 40WT% EMI-TF WITH DIFFERENT THICKNESS (D) UNDER 0.1V STEP VOLTAGE AT 25°C

Membrane thickness (d)	20 m	11 m	1.9 m
Conductivity (S/cm)	9.1×10^{-6}	9.0×10^{-6}	8.6×10^{-6}
Mobility ($cm^2 V^{-1} s^{-1}$)	2.45×10^{-6}	2.37×10^{-6}	2.23×10^{-6}
Debye length D (nm)	0.82	0.81	0.79
Diffusion cof. D ($cm^2 s^{-1}$)	6.28×10^{-8}	6.07×10^{-8}	5.83×10^{-8}
Double layer D_L (s)	1.29×10^{-3}	7.25×10^{-4}	2.49×10^{-4}
Diffusion d_{diff} (s)	15.60	4.86	0.15

In order to analyze the charge storage behavior in the longer time region, we systematically exam the capacitance of the MIM device at its theoretical diffusion time under various applied voltages. Fig. 8 presents the capacitance of the $d=11$ μ m thick device at its diffusion time ($\tau_{diff}=4.86$ seconds) under various applied voltages. It was found that the value of the capacitance does not change much when the applied voltage is below 0.5 V (the error bar is indicated as the dot size in the figure). However, when the applied voltage is larger than 0.5 V, the relationship between the stored charges and the applied voltage becomes nonlinear. The detail of this nonlinear effect needs to be further studied.

IV. CONCLUSION

The influence of the film thickness and applied voltage on the ionic charge dynamics of the Aquivion/EMI-Tf with Au electrodes was investigated. The experimental results indicate that for all the thicknesses studied, the charge dynamics at initial time follow the charging of interfacial capacitors C_D in series with a bulk resistor. For the charge dynamics at times $\gg \tau_{DL}$, the charge dynamics display both applied voltage and thickness d dependence. That is, for the data obtained under 0.1 V, the later stage charging process which is dominated by ion diffusion process seems not to deviate markedly from the d^2 dependence. For voltages > 0.5 V, this later stage charging response does not show d^2 thickness dependence as the gap between the electrodes varies from 1.9 μ m to 20 μ m. Instead, the films with large d can be charged much faster than that predicted from $\tau_{diff}=d^2/(4D)$. On the other hand, when the applied voltage is below 0.5V, the charge storage response is almost linearly proportional to the applied voltage. However, when the applied voltage is larger than 0.5V, the relationship between the stored charges and the applied voltage becomes nonlinear.

ACKNOWLEDGEMENT

The authors would like to express their sincere appreciation to the National Science Council of the Republic of China for supporting this study (NSC 102-2218-E-151-003).

REFERENCES

- [1] W. Lu *et al.*, "Use of ionic liquids for pi-conjugated polymer electrochemical devices," *Science*, vol. 297, pp. 983-987, 2002.
- [2] A. B. McEwen *et al.*, "Electrochemical properties of imidazolium salt electrolytes for electrochemical capacitor applications," *Journal of the Electrochemical Society*, vol. 146, pp. 1687-1695, 1999.
- [3] M. Ue *et al.*, "Application of low-viscosity ionic liquid to the electrolyte of double-layer capacitors," *Journal of the Electrochemical Society*, vol. 150, pp. A499-A502, 2003.
- [4] M. Z. Bazant *et al.*, "Diffuse-charge dynamics in electrochemical systems," *Physical Review E*, vol. 70, pp. 021506-1-021506-24, 2004.
- [5] M. S. Kilic *et al.*, "Steric effects in the dynamics of electrolytes at large applied voltages. I. double-layer charging," *Physical Review E*, vol. 75, pp. 021502-1-021502-16, 2007.
- [6] F. Beunis *et al.*, "Dynamics of charge transport in planar devices," *Physical Review E*, vol. 78, pp. 011502-1-011502-15, 2008.
- [7] F. Beunis *et al.*, "Diffuse double layer charging in nonpolar liquids," *Applied Physics Letters*, vol. 91, pp. 182911-1-182911-3, 2007.
- [8] M. Marescaux *et al.*, "Impact of diffusion layers in strong electrolytes on the transient current," *Physical Review E*, vol. 79, pp. 011502-1-011502-4, 2009.
- [9] F. Strubbe *et al.*, "Generation current of charged micelles in nonaqueous liquids: measurements and simulations," *Journal of Colloid and Interface Science*, vol. 300, pp. 396-403, 2006.

- [10] K. Fukumoto *et al.*, "Room temperature ionic liquids from 20 natural amino acids," *Journal of the American Chemical Society*, vol. 127, pp. 2398-2399, 2005.
- [11] J. G. Huddleston *et al.*, "Characterization and comparison of hydrophilic and hydrophobic room temperature ionic liquids incorporating the imidazolium cation," *Green Chemistry*, vol. 3, pp. 156-164, 2001.
- [12] H. Tokuda *et al.*, "Physicochemical properties and structures of room temperature ionic liquids. 1. variation of anionic species," *Journal of Physical Chemistry B*, vol. 108, pp. 16593-16600, 2004.
- [13] Y. Liu *et al.*, "Ion transport and storage of ionic liquids in ionic polymer conductor network composites," *Applied Physics Letters*, vol. 96, pp. 223503-1-223503-3, 2010.
- [14] S. Liu *et al.*, "Influence of imidazolium-based ionic liquids on the performance of ionic polymer conductor network composite actuators," *Polymer International*, vol. 59, pp. 321-328, 2010.
- [15] J. H. Lin *et al.*, "Charge dynamics and bending actuation in Aquivion membrane swelled with ionic liquids," *Polymer*, vol. 52, pp. 540-546, 2011.
- [16] M. D. Bennett and D. J. Leo, "Ionic liquids as stable solvents for ionic polymer transducers," *Sensors and Actuators a-Physical*, vol. 115, pp. 79-90, 2004.
- [17] M. D. Bennett *et al.*, "A model of charge transport and electromechanical transduction in ionic liquid-swollen Nafion membranes," *Polymer*, vol. 47, pp. 6782-6796, 2006.
- [18] W. Y. Hsu and T. D. Gierke, "Ion-transport and clustering in nafion perfluorinated membranes," *Journal of Membrane Science*, vol. 13, pp. 307-326, 1983.
- [19] A. Ghielmi *et al.*, "Proton exchange membranes based on the short-side-chain perfluorinated ionomer," *Journal of Power Sources*, vol. 145, pp. 108-115, 2005.
- [20] K. D. Kreuer *et al.*, "Short-side-chain proton conducting perfluorosulfonic acid ionomers: why they perform better in PEM fuel cells," *Journal of Power Sources*, vol. 178, pp. 499-509, 2008.
- [21] S. Liu *et al.*, "High electromechanical response of ionic polymer actuators with controlled-morphology aligned carbon nanotube/nafion nanocomposite electrodes," *Advanced Functional Materials*, vol. 20, pp. 3266-3271, 2010.
- [22] S. Liu *et al.*, "Layer-by-layer self-assembled conductor network composites in ionic polymer metal composite actuators with high strain response," *Applied Physics Letters*, vol. 95, pp. 023505-1-023505-3, 2009.
- [23] A. Sergej *et al.*, "Electrode polarization and charge transport at solid interfaces," *Physical Review B*, vol. 80, pp. 184301-1-184301-5, 2009.
- [24] C. Krause *et al.*, "Charge transport and dipolar relaxations in imidazolium-based ionic liquids," *Journal of Physical Chemistry B*, vol. 114, pp. 382-386, 2010.
- [25] C. Wakai *et al.*, "How polar are ionic liquids? determination of the static dielectric constant of an imidazolium-based ionic liquid by microwave dielectric spectroscopy," *Journal of Physical Chemistry B*, vol. 109, pp. 17028-17030, 2005.
- [26] V. Lockett *et al.*, "Differential capacitance of the electrical double layer in imidazolium-based ionic liquids: Influence of potential, cation size, and temperature," *Journal of Physical Chemistry C*, vol. 112, pp. 7486-7495, 2008.



Jun-Hong Lin is an assistant professor of Department of Mold and Die Engineering at National Kaohsiung University of Applied Sciences (R.O.C.). He received his Ph. D. in materials science and engineering from The Pennsylvania State University in 2011. His research focuses on energy related materials and micro forming.